
Identifying and Benchmarking Natural Out-of-Context Prediction Problems

David Madras
University of Toronto
Vector Institute
madras@cs.toronto.edu

Richard Zemel
University of Toronto
Vector Institute
Columbia University
zemel@cs.toronto.edu

Abstract

Deep learning systems frequently fail at out-of-context (OOC) prediction, the problem of making reliable predictions on uncommon or unusual inputs or subgroups of the training distribution. To this end, a number of benchmarks for measuring OOC performance have recently been introduced. In this work, we introduce a framework unifying the literature on OOC performance measurement, and demonstrate how rich auxiliary information can be leveraged to identify candidate sets of OOC examples in existing datasets. We present NOOCH: a suite of naturally-occurring “challenge sets”, and show how varying notions of context can be used to probe specific OOC failure modes. Experimentally, we explore the tradeoffs between various learning approaches on these challenge sets and demonstrate how the choices made in designing OOC benchmarks can yield varying conclusions.

1 Introduction

People often find context useful for prediction, both for improving accuracy and processing efficiency [10]. However, deep learning systems frequently over-rely on context cues [19, 20, 39], which can lead to poor performance on out-of-context (OOC) examples, when contextual information is misleading. By OOC examples, we mean inputs which are uncommon or unusual with respect to the training distribution; these can be thought of as sampled from under-represented subgroups, or low (non-zero) density regions, of the training distribution. OOC is a fundamental problem, a key facet of system robustness. In safety-critical situations, errors can be problematic; as such, it is important to have reliable methods for measuring how well a model can perform OOC. Furthermore, given the rise of larger models and datasets [32], there is a need for scalable approaches to OOC evaluation — even if manual evaluation of “corner cases” by domain experts may (always) be the gold standard.

A key pre-requisite task to *evaluating* OOC performance is *identifying* which examples should be considered OOC. This identification task is a challenging one in and of itself: in a natural image, “context” can be varied, complex and high-dimensional [6, 48, 60, 64]. Therefore, any evaluation method intending to measure a model’s OOC performance must (implicitly) select a specific notion of “OOC performance”. Indeed, since deep learning typically yields underspecified models [14], it is plausible that different choices may yield different measurements. Common approaches include generating semi-synthetic data to simulate the effect of a shift in some salient feature [33, 55, 64], or using some auxiliary information to guide choices about what a reasonable OOC set should be [29, 34].

In this work, we develop a conceptual framework for identifying sets of OOC examples in existing datasets. We show how our framework unifies and generalizes prior literature on OOC performance measurement, and allows us to utilize more complex, structured annotated data to define various formulations of OOC performance. We demonstrate this framework’s effectiveness through uncovering

two OOC “challenge sets” [31] within an existing benchmark, each corresponding to differing notions of context. We show how our framework enables scalable and targeted measurement of models’ OOC performance through clarifying the relationship between the concept of OOC performance and its implementation, allowing for clearer insight on current approaches as well as opportunities for improvement. Our contributions are as follows:

- We present NOOCH (Naturally-Occurring Out-of-context Challenge sets), a suite of challenge sets for evaluating performance on naturally-arising OOC problems, available at <https://github.com/dmadras/nooch>;
- We develop a conceptual framework for automatically identifying OOC challenge sets from existing data by leveraging known underlying structure;
- We demonstrate and contrast two instantiations of this framework using two notions of context, defining concepts of “hard positives” and “hard negatives” in the OOC setting; and
- We quantitatively analyze the performance of several methods from the robust learning literature on these challenge sets, exploring the tradeoffs inherent in different approaches to OOC performance measurement; and qualitatively demonstrate how rich notions of context can yield insight into system robustness.

2 Measuring Out-of-Context Performance

Intuitively, a model which has good OOC performance should be able to maintain good performance under unusual or perturbed contextual conditions. We distinguish this from the out-of-distribution (OOD) problem [28], which is usually concerned with inputs from a different domain than the training set. Rather, the OOC prediction problem is more similar to subgroup robustness or distributional shift, where a model must perform well on uncommon input regions at training time. However, even after drawing this distinction, the notion is ill-defined: context may refer to concepts as varied as object relationships [60], image backgrounds [64], experimental settings [48], or world models [6]. Furthermore, even fixing a notion of context, the criterion for what should make something out-of-context (OOC) is still unclear. For instance, Peters et al. [48] focus on previously unobserved contexts (i.e. environments), whereas Xiao et al. [64] are concerned with unusual contexts given the class of interest (i.e. perturbations to image background).

Clearly, defining a benchmark to measure a method’s OOC performance requires a number of design choices, which has fostered a recent proliferation of OOC benchmarks. We note in particular, one of the key choices is around the usage of *auxiliary information*. Across the literature on OOC performance measurement, there are a plethora of approaches to defining OOC criteria using some type of auxiliary information C . For the purposes of algorithm design, C may be assumed to be available at training, validation, and/or test time, or not at all — however, at the time of benchmark design, it is available on a sufficiently large portion of the collected dataset to guide the designers’ choices about what a suitable OOC criterion should be. Examining the current literature on measuring OOC performance, we identify the following as a unifying framework:

1. Identify some existing auxiliary information C , a variable which takes some value on many (or all) examples and specifies some underlying structure in the data.
2. Select a notion of “OOC” (e.g. “images with misleading backgrounds are OOC”, “examples from unfamiliar time periods are OOC”) and define an “OOC criterion” by choosing a binary function ϕ of C .
3. Restrict the test set to those examples where $\phi = 1$. Optionally, also restrict the training set to those examples where $\phi = 0$.

We show in Table 1 how a range of prior literature leverages auxiliary information to define OOC criteria. We can think of C as providing benchmark designers with some type of “inductive bias” around what should be considered OOC for a given benchmark. The above framework implies that there is a diversity of OOC criteria which can be defined over any dataset, and this class is as broad as the class of functions ϕ which can be defined over the available auxiliary information. In the rest of the paper, we take advantage of the flexibility of this framework to give two examples of such an approach. We show that by leveraging more complex annotated structure, we can create multiple OOC benchmarks from an existing dataset using multiple criteria for what should be considered “OOC”.

Dataset	Auxiliary Information C	OOO function ϕ
Waterbirds [55]	1 if background is water (binary)	$C \neq Y$
iWildCam2020-Wilds[34]	camera trap ID (categorical)	$C \notin \{1 \dots 245\}$
FMoW-Wilds [34]	time stamp (ordinal)	$C_{time} \geq 2013$
Imagenet-A [29]	max NLL of ensemble (continuous)	$C \geq -\log(0.15)$
Breeds [56]	subclass (categorical)	$C \in \text{target subset}$

Table 1: Examples of OOC benchmarks from the literature under our framework. The right-most column lists the condition under which $\phi = 1$. The OOC function ϕ in [29] has several additional filtering steps, some heavily manual.

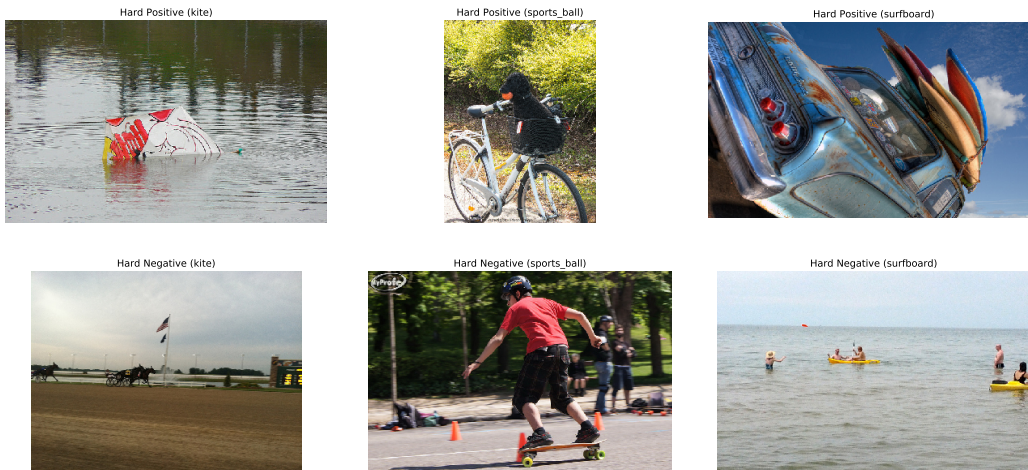


Figure 1: Using the co-occurrence/extractability (CE) criterion, examples of (0.05, 0.1)-hard positives (top row) and negatives (bottom row) for the classes (L to R): kite, sports_ball, surfboard.

We trace out how the choices made in designing these criteria correspond to different notions of context, and demonstrate experimentally that these yield varying measurements of OOC performance.

3 Finding Naturally-Occurring OOC Problems

In this section, we demonstrate concretely how rich auxiliary information can be used to study the way that context shifts arise naturally within an existing computer vision benchmark, and provide two criteria for OOC performance that can be computed from these annotations. Throughout, we consider the binary prediction task of determining object presence, a problem where relationships between various objects naturally provide helpful context — given an image X , is an object of class Y present or not?

3.1 Background: COCO and COCO-Stuff

The Microsoft Common Objects in COntext dataset (COCO) [37] is a computer vision dataset consisting of images of natural scenes. Each image is annotated with instance labels and segmentations for every “thing” in the image, as well as several captions describing the content of the scene. Images usually contain multiple items and as such usually have multiple labels.

However, for the purposes of investigating OOC prediction, many relevant objects are not labelled in COCO; for instance, background objects such as “sky” or “grass” are not COCO classes. Fortunately, the COCO-Stuff dataset [7] provides labels and segmentations for all of the “stuff” in the images from COCO. The “thing” vs “stuff” distinction is a technical one: a thing is an object with a specified size and shape, whereas stuff has no “defined spatial extent” [17]. Having both thing and stuff labels is essential for understanding model behaviour on OOC examples, since it is exactly these “stuff” classes which often (but not always) provide important context cues. Taken together, the thing and stuff annotations yield a rich sandbox for queries about the role of context in prediction. For our



Figure 2: To contrast the CE and Gist criteria, we show samples from the airplane (L) and bowl (R) tasks.

purposes, COCO-Stuff contains 171 binary tasks for determining object presence (81 thing classes and 90 stuff classes; we ignore the 1 “unlabelled” class).

3.2 Automatically Identifying OOC Examples: Hard Positives and Negatives

Here, we consider two contrasting notions of “OOO”: 1. the presence/absence of frequently co-occurring, easily extractible objects; and 2. an unusual “gist” of a scene. We define these two notions of context below, presenting two criteria for identifying naturally-occurring OOC prediction problems within the existing COCO(-Stuff) dataset, and discussing how we can use annotations as proxies to define an OOC indicator ϕ . We identify two types of OOC examples: *hard positives*, where the class is present despite an unusual context, and *hard negatives*, where the class is *not* present, despite a usual context.

3.2.1 Defining Context Using Co-Occurrences and Extractibility

For an object class Y , context cues often come in the form of another object class C that has two properties (cf. [39]). First, C and Y co-occur frequently [5]. Second, C is more *extractible* than Y — easier to detect. If C were *less* extractible than Y it would not be a useful cue for detecting Y , as a model could detect Y directly.

We can utilize these properties to create candidate context cues C for a class of interest Y . Given segmentations, we can use an object’s size within an image as a proxy for extractibility (larger objects tend to be more extractible). Let the *Area* operator take the sum of the areas of all segmentations of instances of that object, or return 0 if the object is not present. Then, to estimate from the training set how important of a context variable C is, we can compute $A(C, Y) = \mathbb{E}[Area(C) - Area(Y) | Y = 1]$. When $A(C, Y)$ is larger, this means that when Y is present, C is usually also present, and on average, takes up more of the image than Y does. When $A(C, Y) > \alpha$, we say that C is an α -strong context cue for Y (or just α -context for brevity). We find that many of the contexts identified using this method for large enough α are intuitive. Some examples of (label, 0.05-context) pairs are: (car, road), (bowl, dining_table), (cow, grass).

Using this notion of context, we can then define hard positive and hard negative examples. We make the simplifying *noisy-or* assumption: that each context cue provides evidence for Y , so that the presence of any cue supports Y being present, while the absence of all provides evidence against Y ’s presence. Given some image, we can define an (α, β) -hard positive or negative. If $Y = 1$, and for all α -context cues C , we have $Area(C) < \beta$ in this image (and there is at least one α -context cue), then the example is an (α, β) -hard positive. Alternatively, if $Y = 0$, and there exists some α -context variable C such that $Area(C) > \beta$, then the example is an (α, β) -hard negative. We will call this method the co-occurrence/extractibility (CE) criterion (see Fig 1 for examples). Throughout, we use $\alpha = 0.05, \beta = 1$ unless otherwise noted; these parameters were chosen since they approximately equalize $P[(X, Y) \text{ is } (\alpha, \beta)\text{-hard} | Y = y]$ across $y = 0, 1$. See Appendix B for more details.

3.2.2 Defining Context Using Gist

We now turn to a broader notion of context, that of the “gist” of a scene [60], or its overall semantic content. This is something that humans can recognize easily [36], but goes beyond object frequency and extractibility. When an object is present in a scene whose gist is very different from the scenes the object was present in at training time, this may make prediction difficult.

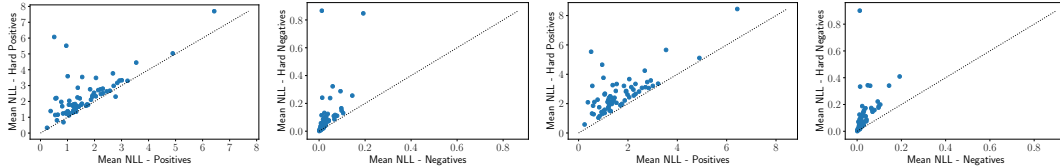


Figure 3: We find that hard positives/negatives induce higher average loss for both criteria. Each point is a task in COCO-Stuff: the x- and y-axis values show the average loss achieved by an ERM model on all positives (negatives) and the average loss on hard positives (negatives). From L to R: CE criterion (positives), CE criterion (negatives), gist criterion (positives), gist criterion (negatives). The diagonal line represents where the hard example losses match marginal losses.

We describe our method for estimating gist shift, which we call the gist criterion. We use caption annotation data in COCO (each image has 5 caption sentences), making the assumption that information in a caption captures the gist of a scene. We then take an SBERT embedding [49] of each image caption for an image, and average these embeddings to get a single embedding for that image. Then, for a given image and some target label Y , we find the cosine similarity between that image’s embedding and the average embedding across all training images with $Y = 1$. If this similarity is below some threshold τ , and $Y = 1$ for the test image, it is a τ -hard positive; if this similarity is above τ , and $Y = 0$ for the test image, it is a τ -hard negative. Note, we do not look at distance to $Y = 0$ examples; we assume that captions for $Y = 0$ images may have little in common, whereas the mean caption for $Y = 1$ is a prototypical description of Y “in context”. Throughout, we set the threshold τ for each task so that the number of hard positives and negatives is the same as the CE criterion for that task, to facilitate comparisons. See Figure 2 for examples of hard positive and negatives chosen by this criterion in comparison to the CE criterion, and Appendix B for more details.

3.3 NOOCH-CE and NOOCH-Gist: Selecting Challenge Sets

We train binary classifiers to minimize average NLL on each of the 171 classes in COCO-Stuff. We find that for nearly all tasks, the hard positives and negatives defined by our methods incur higher average loss than positive and negative examples respectively (Fig. 3), for both the CE and Gist criteria. This provides some evidence that our criteria are, in fact, identifying examples which are more difficult to classify correctly.

To select candidate OOC tasks for our challenge sets, we select the 12 tasks with the largest difference between average NLL on hard examples (by the CE criterion) and average NLL on all examples, filtering out those tasks without at least 50 hard positives and hard negatives. We call these tasks the NOOCH (Naturally-Occurring Out-of-context Challenge) suite. We then identify two groups of challenge sets: NOOCH-CE, which consists of the hard positive and negative examples on each of the 12 tasks in NOOCH as identified by the CE criterion; and NOOCH-Gist, which is the analogous set for the gist criterion; see Table 2 for a list of tasks. This gives us 24 total challenge sets on which to evaluate an ML model’s OOC performance.

Task	# Hard +	# Hard -	# +
car	1539	949	2585
bowl	944	1084	1463
boat	361	756	649
fire-hydrant	189	1577	332
airplane	258	3622	635
cow	194	2360	445
backpack	607	6413	1183
cup	743	6852	1926
surfboard	147	4011	750
tie	136	6347	778
sports-ball	151	6574	860
kite	55	6725	451

Table 2: Counts of hard positive, hard negative & positive examples in the test set per NOOCH task.

Contrasting the Two Criteria (Fig. 2). The left two images in Fig. 2 are hard positives on the airplane task. On the far left, we see the inside of an airplane: this is selected as a hard positive by the CE criteria because there is no sky visible. On the second left, the sky is visible but the overall scene is unusual; this is a hard positive by the Gist criteria. The right two images are hard negatives on the bowl task. On the second right, we see a large dinner with many plates: this is a hard negative by the CE criteria because there is a prominent

dining table but no bowls. On the far right, we see a paper plate on a desk (not a dining table): this is a hard negative by the Gist criteria since there is no bowl but it is similar to images where you might expect a bowl.

4 Evaluating Robustness Approaches on NOOCH

We now turn to evaluating various ML methods on the NOOCH benchmarks. We choose to focus on four categories of methods which provide a useful contrast between different approaches to OOC prediction. Expected risk minimization (**ERM**) is the standard loss function in ML systems; as shown by Gulrajani and Lopez-Paz [21], it can be difficult to beat on domain generalization problems. Label-based adjustments (**Reweight** and **US**) use information about label imbalance at training time to adjust the loss function towards performing better on unusual labels. Environment-based methods (**GDRO** [55], **IRM** [2], **Reweight-Envs**, **US-Envs**) use categorical auxiliary information (i.e. *environments*) at training time to adjust the loss function towards performing better on unusual subgroups. Finally, adaptive methods (**CVaR** ([50]) and **Focal** [38]) do not use auxiliary information at all, but instead try to infer adaptively from the input during training what the worst-performing subgroups should be. See App. A for information on other methods we experimented with but did not include here. We found the methods we included here had the best results overall, on the standard and hard examples.

Throughout, we use the following notation. We are given a dataset $\{x_i, y_i\}_{i=1}^n$ with inputs and target labels respectively, and possibly some side information $\{c_i\}_{i=1}^n$ as well (e.g. environment variables). If side information is available, we assume it is available at training time but not necessarily test time. We are aiming to learn a function $f : \mathbb{X} \rightarrow \mathbb{Y}$. We assume ℓ to be the the example-wise cross-entropy loss function.

4.1 Expected Risk Minimization

Expected risk minimization (ERM) is the standard paradigm for training ML models. In ERM, we minimize the mean loss ℓ on the training set, plus potentially some data-independent regularizer \mathcal{R} :

$$\mathcal{L}_{ERM}(f) = \frac{1}{n} \sum_{i=1}^n \ell(f(x_i), y_i) + \mathcal{R}(f) \tag{1}$$

4.2 Label-Based Adjustments

Since COCO-Stuff contains significant label imbalance, we consider methods intended to correct for label imbalance. We let $w_i = P(Y = y_i)$ in the training set. To make a fairer comparison with the environment-based methods (below), we add a tuning parameter α to control the degree of adjustment. $\alpha = 1$ represents the standard versions of these loss functions, but we frequently found other values $\alpha \in [0, 2]$ to be useful.

Label Reweighting. We reweight the loss of each training example in the ERM loss function, inversely proportional (when $\alpha = 1$) to the likelihood of observing that label:

$$\mathcal{L}_{Reweight}(f) = \frac{1}{n} \sum_{i=1}^n \left(\frac{1}{w_i}\right)^\alpha \ell(f(x_i), y_i) + \mathcal{R}(f) \tag{2}$$

Label Undersampling. Rather than sampling training examples uniformly, we sample them with probability inversely proportional (when $\alpha = 1$) to the likelihood of observing that label. We let \mathcal{I} be a list of indices of size n , sampled independently from $[1 \dots n]$, such that for each $j \in \mathcal{I}$, $P(j = i)$ is proportional to $(\frac{1}{w_i})^\alpha$. We redraw this for the training set every epoch and weight their losses equally as follows:

$$\mathcal{L}_{Undersampling}(f) = \frac{1}{n} \sum_{i \in \mathcal{I}} \ell(f(x_i), y_i) + \mathcal{R}(f) \tag{3}$$

4.3 Environment-Based Methods

One common setting is where the auxiliary information c_i for each example is a categorical variable, representing an *environment*. The notion of environments for robust learning was originally given with causal motivation [48], where each value of c represents a different intervention on the underlying causal graph. However, this type of grouping procedure can be used completely separately from the causal context, and so we just consider it to represent some informative partition of our data, which is defined as an input at training time. Here, $c \in \{1 \dots C\}$ is an integer and we use the following shorthand to describe the average loss for an environment, with n_c referring to the number of examples in that environment:

$$\ell_c(f) = \frac{1}{n_c} \sum_{i=1}^n \ell(f(x_i), y_i) \mathbb{1}\{c_i = c\} \quad (4)$$

Group DRO. The first environment-based method we consider is Group Distributionally Robust Optimization (GDRO) [55], which aims to minimize the loss on the worst of C partitions, with partition c of size n_c , and group adjustment hyperparameter K :

$$\mathcal{L}_{GDRO}(f) = \max_{c \in \{1 \dots C\}} \left\{ \ell_c(f) + \frac{K}{\sqrt{n_c}} \right\} + \mathcal{R}(f) \quad (5)$$

This loss aims to ensure that no group’s loss is that bad, and the group adjustment term ensures greater focus on smaller groups, which may otherwise be ignored.

IRM. The second environment-based method we consider is invariant risk minimization (IRM) [2]:

$$\mathcal{L}_{IRM}(f) = \sum_{c=1}^C \ell_c(f) + \lambda \|\nabla_w|_{w=1} \ell_c(w \cdot f)\| + \mathcal{R}(f) \quad (6)$$

The second term here is a gradient penalty on the output of f , w is a constant multiplier on the output of f , and λ is a hyperparameter. The intuition for this is somewhat involved [2]; the overarching motivation is that each environment should learn a representation such that the same predictive classifier is optimal across environments.

Environment Reweighting and Undersampling. These are equivalent to label reweighting/undersampling above, but with $w_i = P(C = c_i)$.

4.4 Adaptive Methods

Finally, we consider a class of loss functions which, rather than using an injection of side information to specify which examples are OOC, focuses dynamically on the hardest examples at each step. The first is conditional variance-at-risk optimization (CVaR). This can be cast as a type of distributionally robust optimization (DRO) [16], where we aim to minimize the loss over, rather than the whole training set, a worst-case distribution over training examples. For some $p \in (0, 1)$, $\text{CVaR}(p)$ is defined as the average loss of the p -percent worst-loss examples.

We also consider focal loss [38], which dynamically upweights high loss examples using a parameter $\gamma \geq 0$. With binary y , $q(x, y) = f(x)$ if $y = 1$ and $q(x) = 1 - f(x)$ if $y = 0$, with $f(x) \in [0, 1]$ as the continuous-scored output of f , not the binary prediction. Then, we have focal loss as a modification of the cross-entropy loss — at $\gamma = 0$ this reduces to cross-entropy; as γ increases, it focuses more loss on the examples which have higher loss already:

$$\mathcal{L}_{Focal}(f) = \frac{1}{n} \sum_{i=1}^n -(1 - q(x_i, y))^\gamma \log(q(x_i, y)) + \mathcal{R}(f) \quad (7)$$

5 Related Work

A range of datasets have been proposed for the purposes of benchmarking OOC prediction. Several focus on realistic OOC prediction: WILDS [34] contains problems from across a range of applications;

Imagenet-A [29] select examples which perform worst on an ensemble of models; ObjectNet [4] focuses on object recognition and shows objects varied by a range of attributes; Choi et al. [8] isolate 26 images of objects in unusual contexts from a larger dataset. Our work functions well as a complement to any of these datasets; we believe it is novel due to our ideas for scalably identifying challenge sets from annotated data, as well as its delineation of hard positives and hard negatives. The notion of “challenge sets” [31], “stress tests” [42], or “contrast sets” [18] from the NLP literature is an inspiration for our work as well. A range of primarily semi-synthetic datasets include those that center around: image corruption (Imagenet-C, Imagenet-P [27]; Pascal-C, Coco-C, Cityscapes-C [40]); object hierarchy (BREEDS [56]); synthetic shifts in background (Waterbirds [55]; Imagenet-9 [64]); color (Colored MNIST [2, 33]); a group attribute (partitioned Civil Comments [1]); or purely synthetic data (Invariance Unit Tests [3]).

Several works have discussed explicit examples where deep models failed to perform OOC prediction in practice. Oakden-Rayner et al. [45] and Winkler et al. [62] discuss the risk of this occurring in the medical domain, and Shetty et al. [58] in the autonomous driving domain. Other works have detailed the challenge of OOC prediction for deep models, using frames of “shortcuts” [20], “simplicity” [57], “extractibility” [39], texture biases in CNNs [19], or the challenge of out-of-place objects [51].

A range of work outside deep learning considers the OOC prediction problem from a different direction, focusing on how to improve prediction by taking context into account [9, 26, 41, 66]. Other work looks at the idea of using a latent variable to represent scene gist [46, 63]. A number of newer methods not discussed elsewhere in the paper also aim to solve the OOC problem, including those that involve side information [30, 35, 59, 65], those that involve side information through causal underpinnings [25, 53], and those that ignore side information altogether [12, 13, 15].

6 Experiments

In this section, we compare and contrast the various measurements of OOC performance yielded by NOOCH, along with the semi-synthetic Waterbirds dataset [55]. For all experiments we use a ResNet-50 [24], finetuned from ImageNet-pretrained features [54]. See App. B and C for further experimental details. For the environment-based methods, we follow Sagawa et al. [55] and create 4 environments: 1 for each element of the cross-product of the label and its highest- α context class. Many of the robust baselines from Sec. 4 come with a hyperparameter which aims to trade off between average performance and OOC performance; we choose the hyperparameter which minimizes the maximum loss of hard positives and hard negatives on the validation set.

6.1 Quantitative Analysis

6.1.1 Main Results: Different Criteria Yield Different Evaluations

In Tables 3 and 4, we show AUC (area under the ROC curve) on hard examples for each method we focus on and each of the 12 NOOCH tasks individually. We choose AUC as a metric since it is robust to label imbalance, and tasks in NOOCH contain 1-10% positive examples.

For comparison, we show in Table 5 an analogous table of results for Waterbirds [55], a semi-synthetic dataset which is generated by pasting images of birds on top of either land or water backgrounds; the goal is to classify land birds from water birds. At training time, land birds are mostly shown on land (and water birds on water), but at test time we hope to perform well, regardless of background. The information regarding place is made available through environments: the four environments are land/land, land/water, etc. For Waterbirds, we show both AUC-Hard (our metric) and worst-group error/NLL (the metrics from Sagawa et al. [55]).

Environments are More Useful on Simpler Benchmarks. We first note that the three different benchmarks presented yield varying conclusions about the methods in question; in particular, the relative performance of the best environment-based methods vary greatly between the benchmarks. We find that environment-based methods perform better on the benchmarks where the structure of the shift (i.e. the form of ϕ) is better specified by the environments. In Table 5, we see that there is a particularly large gap in performance between the best environment-based methods (particularly GDRO) and the methods that do not use environments. For instance, GDRO and IRM improve over ERM by about 0.3 in worst-group error (the metric of choice in Sagawa et al. [55]); and GDRO

Task	ERM	CVaR	Focal	Reweight	US	Reweight (Envs)	US (Envs)	GDRO	IRM
car	0.769	0.787	0.759	0.773	0.773	0.886	0.846	0.891	0.868
bowl	0.749	0.781	0.734	0.751	0.759	0.864	0.814	0.865	0.828
boat	0.869	0.888	0.823	0.866	0.877	0.954	0.923	0.945	0.925
fire-hydrant	0.913	0.933	0.908	0.927	0.913	0.933	0.920	0.946	0.942
airplane	0.986	0.984	0.983	0.986	0.985	0.991	0.986	0.991	0.986
cow	0.935	0.937	0.932	0.939	0.938	0.963	0.948	0.963	0.943
backpack	0.812	0.806	0.809	0.816	0.812	0.813	0.816	0.871	0.844
cup	0.870	0.863	0.867	0.876	0.873	0.879	0.875	0.825	0.869
surfboard	0.939	0.947	0.933	0.940	0.939	0.960	0.940	0.960	0.957
tie	0.742	0.752	0.728	0.760	0.763	0.756	0.761	0.806	0.775
sports-ball	0.867	0.869	0.871	0.869	0.868	0.911	0.890	0.911	0.894
kite	0.932	0.932	0.937	0.940	0.928	0.949	0.936	0.960	0.950
Average	0.865	0.873	0.857	0.870	0.869	0.905	0.888	0.911	0.899

Table 3: AUC on hard test examples for all 12 NOOCH-CE stress tests, after hyperparameter selection. Bold numbers have overlapping standard deviations with the highest observed mean’s.

Task	ERM	CVaR	Focal	Reweight	US	Reweight (Envs)	US (Envs)	GDRO	IRM
car	0.766	0.785	0.763	0.768	0.773	0.845	0.823	0.863	0.832
bowl	0.642	0.686	0.635	0.656	0.678	0.692	0.698	0.704	0.670
boat	0.826	0.855	0.771	0.823	0.823	0.897	0.868	0.884	0.872
fire-hydrant	0.840	0.865	0.822	0.849	0.841	0.834	0.836	0.823	0.845
airplane	0.977	0.979	0.975	0.978	0.976	0.978	0.977	0.981	0.977
cow	0.901	0.912	0.877	0.903	0.906	0.908	0.908	0.911	0.896
backpack	0.716	0.717	0.725	0.731	0.749	0.729	0.736	0.732	0.750
cup	0.733	0.738	0.727	0.735	0.742	0.759	0.771	0.742	0.755
surfboard	0.913	0.920	0.900	0.912	0.914	0.909	0.912	0.882	0.894
tie	0.822	0.816	0.813	0.829	0.824	0.829	0.831	0.835	0.840
sports-ball	0.830	0.832	0.828	0.830	0.822	0.866	0.859	0.880	0.855
kite	0.942	0.939	0.945	0.947	0.936	0.947	0.939	0.947	0.943
Average	0.826	0.837	0.815	0.830	0.832	0.849	0.847	0.849	0.844

Table 4: AUC on hard test examples for all 12 NOOCH-Gist stress tests, after hyperparameter selection. Bold numbers have overlapping standard deviations with the highest observed mean’s.

Metric	ERM	CVaR	Focal	Reweight	US	Reweight (Envs)	US (Envs)	GDRO	IRM
Worst-Group Error	0.4	0.354	0.402	0.361	0.336	0.233	0.146	0.108	0.127
Worst-Group NLL	1.03	0.657	0.722	0.884	0.883	0.535	0.417	0.306	0.346
AUC-Hard	0.691	0.703	0.506	0.657	0.701	0.744	0.778	0.929	0.788

Table 5: AUC on “hard” test examples on the Waterbirds dataset. Hard examples are the union of two groups: land birds on water backgrounds and water birds on land backgrounds. Worst-group error or NLL takes the worse of the two; AUC-Hard calculates the AUC across the union.

improves over *all* other methods by about 0.14 in AUC on hard examples. This difference is an order of magnitude greater than observed on either NOOCH benchmark, suggesting that semi-synthetic datasets (such as Waterbirds), may overestimate the performance of current environment-based methods, and possibly GDRO in particular.

We see a smaller version of this phenomenon when just comparing NOOCH-CE to NOOCH-Gist: the environment-based methods are also the ones whose performance falls off the most between NOOCH-CE and NOOCH-Gist. This could be because NOOCH-CE is a simpler benchmark, more well specified by the given environments. The contrast between Tables 3, 4 and Table 5 documents the usefulness of having benchmarks for robustness across a range of complexity, and motivates the creation of benchmarks such as NOOCH.

Gist Shift is Difficult. We further note that performance on NOOCH-Gist is worse than on NOOCH-CE. This suggests that the more complex notion of context embodied by the gist yields a more difficult OOC task. In some ways, would expect models to find these more holistic shifts harder, as these gist shifts go well beyond “shortcuts” [20]. We also note that the gap between the environment-based methods and ERM is much smaller on NOOCH-Gist, indicating that ERM is a strong baseline on this task, making gist shift a useful direction for OOC prediction research.

Access to Auxiliary Information is More Important than Algorithm. Overall, environment-based methods perform the best on all three benchmarks — we expect this to be the case, since these

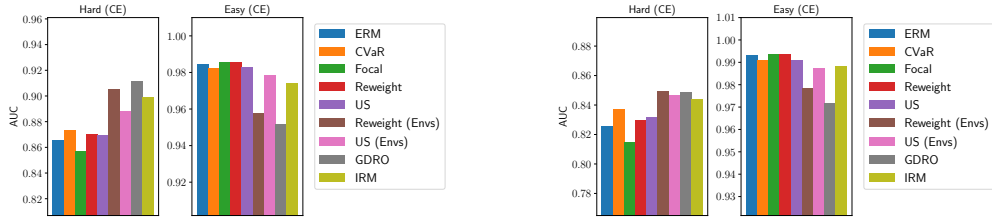


Figure 4: AUC (area under the ROC curve) achieved on hard and easy examples. Higher is better.

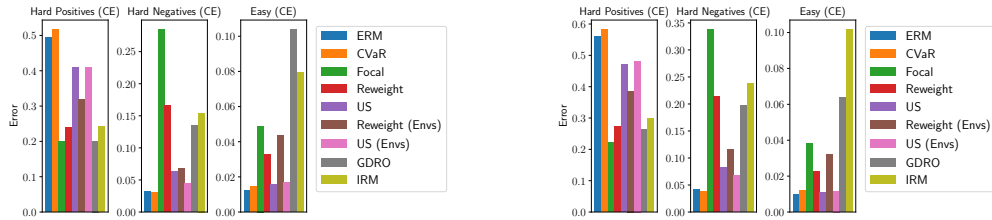


Figure 5: Classification error achieved on hard positive, hard negative, and easy examples.

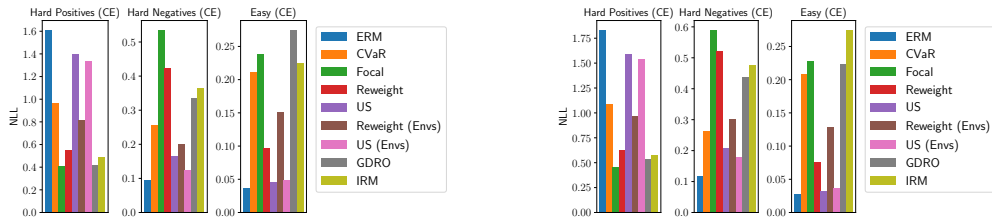


Figure 6: Negative log-likelihood (NLL) achieved on hard positive, hard negative, and easy examples.

methods are given access to structure which is relevant to the OOC task at hand. This is mostly clearly indicated in the improvement between reweighting/undersampling methods when using environments rather than labels. Interestingly, we find that on the more complex NOOCH benchmarks, reweighting examples by environment performs similarly to more specialized methods such as GDRO/IRM, given an equivalent amount of hyperparameter tuning. This is true to a lesser degree for undersampling by environment as well. This suggests that current environment-based methods have significant room to improve when it comes to more complex OOC benchmarks.

6.1.2 Secondary Observations

In Figures 4, 5, 6, and 7, we show AUC, classification error, mean negative log-likelihood (NLL), and expected calibration error (ECE) [22] respectively, averaged across the 12 tasks. For AUC and ECE, we display results for hard and easy examples separately (where an “easy” example is defined as one which is not “hard”, i.e. not a hard positive or hard negative). For error and NLL, we further break out the results on hard examples into hard positives and hard negatives. For all, we show NOOCH-CE (L) and NOOCH-Gist (R) separately.

Tradeoffs Exist Between Harder and Easier Examples. We note two tradeoffs across AUC, error, and NLL results: models that are better on hard examples tend to be worse on easy examples (and vice versa), and models that are better on hard positives tend to be worse on hard negatives. ERM is better on easy examples and hard negatives: since the dataset is imbalanced, the hard negatives are the easier “hard” examples, and we expect ERM to perform better here since negatives are the majority class.

Adaptive Methods Find Different Tradeoffs. We find that CVaR and focal loss find interesting tradeoffs between ERM and environment-based methods. CVaR performs comparably to ERM on both hard and easy examples by AUC and error measures; and by ECE it is by far the worst of



Figure 7: Expected Calibration Error (ECE) achieved on hard and easy examples. Lower is better.

any method. However, CVaR’s NLL on hard positives is between ERM and the environment-based methods’. Focal loss, on the other hand, performs similarly to ERM by AUC on both hard and easy examples, but it performs similarly to the environment-based methods on hard positives and negatives by error and NLL, providing a strong tradeoff between overall and OOC performance.



Figure 8: Test set examples where GDRO most improves over ERM (L) hard positives and (R) hard negatives from the NOOCH-CE car category. Titles show NLL for each method on that image.

negatives (in NOOCH-CE). The hard positive and hard negative where GDRO most overperformed are both images we might expect, where the object label and context do not match: a living room with a tiny toy car on the shelf, and a normal street scene that happens to not have any cars. See App. D for analysis on where GDRO underperforms ERM.

Contrasting NOOCH-CE and NOOCH-Gist. In Fig. 9, we use examples of hard positives from the cow task to contrast the CE and gist criteria. On the left, we show a hard positive from NOOCH-CE, with cows standing on pavement: this is a hard positive in NOOCH-CE since there is no grass; GDRO and IRM outperform ERM on this image. However, it is *not* a hard positive in NOOCH-Gist, since cows are the central focus of the image. On the right, we show a hard positive from NOOCH-Gist, where the image focuses on a giraffe, but there are several white cows in the background standing on a grassy field. This is *not* a hard positive in NOOCH-CE, due to the large field, but it *is* a hard positive in NOOCH-Gist, since the giraffe is the focus of the image. ERM outperforms GDRO and IRM on this image — the environment-based objectives do not encourage as strong performance where the context (grass) and object (cow) align.

7 Discussion

Limitations & Impacts. The idea of computationally identifying OOC examples is necessarily limited: by their nature, OOC examples are exceptions to rules, and there will always be OOC examples which can only be discovered through qualitative examination. Further, the task chosen for our benchmark was chosen for simplicity of analysis in a research context rather than real world significance — outputting segmentations or many-way classification may be more applicable to most applications. We hope that the impact of our work is to enable better evaluation of model performance

Two Surprising Calibration Results. We found that there was *not* the same tradeoff with calibration as there was with the other metrics. In particular, ERM and undersampling had the best calibration on *both* hard and easy examples, suggesting there may be a path forward to avoid some of the tradeoffs between OOC and average performance by thinking more about calibration. Secondly, we found the environment-based methods were not better calibrated, even on hard examples.

6.2 Qualitative Analysis

Where Environment-based Learning Improves Over ERM. In Fig. 8, we show the images with the largest gaps in NLL on the car task among two groups: hard positives and hard

on atypical or under-represented examples, both through usage of these challenge sets and ones inspired by the ideas presented here. However, the usage of benchmarks can have downsides where standardized performance metrics are prioritized over fundamental advances in modelling which are not captured in those metrics. In various applications of interest, results may need to be reported across a number of different metrics since this gives a clearer picture of model performance — AUC may not always be a (or the most) relevant metric.



Figure 9: Examples of hard positives from NOOCH-CE (L) and NOOCH-Gist (R) for the cow task. Titles show NLL for several methods on that image.

Conclusion & Looking Forward.

In this work, we study OOC evaluation as its own field, drawing attention to the range of evaluation schemes which can be used and the ways in which they may differ. We demonstrate that using auxiliary structure in the data can be a useful means of defining context, and that this structure can be used in rich ways to identify various faces of the OOC problem. Through this exploration, we find that methods which take advantage of auxiliary information may be more generously evaluated by OOC benchmarks

which more are cleanly defined by that information.

In closing, we would like to highlight the idea systematizing OOC evaluation, whether this is through automatic discovery of OOC examples through annotations or some other means. This not only enables the scalable creation of challenge sets, but allows for faster generation and exploration of new hypotheses about the type of context shifts that models struggle on, possibly analogous to automatic test generation in the debugging literature [11, 43]. We hope that methods of this type can be applied elsewhere to better understand the challenges of OOC prediction.

Acknowledgments and Disclosure of Funding

Thanks to Marc-Etienne Brunet, Eleni Triantafylliou and Elliot Creager for their helpful thoughts on the manuscript, as well as to four anonymous reviewers for useful feedback. David Madras was supported by an NSERC Alexander Graham Bell Canada Graduate Scholarship-Doctoral (CGS-D). Resources used in preparing this research were provided, in part, by the Province of Ontario, the Government of Canada through CIFAR, and companies sponsoring the Vector Institute (www.vectorinstitute.ai/#partners).

References

- [1] R. Adragna, E. Creager, D. Madras, and R. Zemel. Fairness and robustness in invariant learning: A case study in toxicity classification. *arXiv preprint arXiv:2011.06485*, 2020.
- [2] M. Arjovsky, L. Bottou, I. Gulrajani, and D. Lopez-Paz. Invariant risk minimization. *arXiv preprint arXiv:1907.02893*, 2019.
- [3] B. Aubin, A. Słowik, M. Arjovsky, L. Bottou, and D. Lopez-Paz. Linear unit-tests for invariance discovery. *arXiv preprint arXiv:2102.10867*, 2021.
- [4] A. Barbu, D. Mayo, J. Alverio, W. Luo, C. Wang, D. Gutfreund, J. Tenenbaum, and B. Katz. Objectnet: A large-scale bias-controlled dataset for pushing the limits of object recognition models. *Advances in neural information processing systems*, 32:9453–9463, 2019.
- [5] I. Biederman, R. J. Mezzanotte, and J. C. Rabinowitz. Scene perception: Detecting and judging objects undergoing relational violations. *Cognitive psychology*, 14(2):143–177, 1982.
- [6] A. Bobick and C. Pinhanez. Using approximate models as source of contextual information for vision processing. In *Proc. of the ICCV*, volume 95, pages 13–21. Citeseer, 1995.

- [7] H. Caesar, J. Uijlings, and V. Ferrari. Coco-stuff: Thing and stuff classes in context. In *Proceedings of the IEEE conference on computer vision and pattern recognition*, pages 1209–1218, 2018.
- [8] M. J. Choi, A. Torralba, and A. S. Willsky. A tree-based context model for object recognition. *IEEE transactions on pattern analysis and machine intelligence*, 34(2):240–252, 2011.
- [9] M. J. Choi, A. Torralba, and A. S. Willsky. Context models and out-of-context objects. *Pattern Recognition Letters*, 33(7):853–862, 2012.
- [10] M. M. Chun. Contextual cueing of visual attention. *Trends in cognitive sciences*, 4(5):170–178, 2000.
- [11] D. M. Cohen, S. R. Dalal, J. Parelius, and G. C. Patton. The combinatorial design approach to automatic test generation. *IEEE software*, 13(5):83–88, 1996.
- [12] E. Creager, J.-H. Jacobsen, and R. Zemel. Environment inference for invariant learning. In *ICML Workshop on Uncertainty and Robustness*, 2020.
- [13] N. Dagaev, B. D. Roads, X. Luo, D. N. Barry, K. R. Patil, and B. C. Love. A too-good-to-be-true prior to reduce shortcut reliance. *arXiv preprint arXiv:2102.06406*, 2021.
- [14] A. D’Amour, K. Heller, D. Moldovan, B. Adlam, B. Alipanahi, A. Beutel, C. Chen, J. Deaton, J. Eisenstein, M. D. Hoffman, et al. Underspecification presents challenges for credibility in modern machine learning. *arXiv preprint arXiv:2011.03395*, 2020.
- [15] J. Duchi and H. Namkoong. Variance-based regularization with convex objectives. *arXiv preprint arXiv:1610.02581*, 2016.
- [16] J. C. Duchi, P. W. Glynn, and H. Namkoong. Statistics of robust optimization: A generalized empirical likelihood approach. *Mathematics of Operations Research*, 2021.
- [17] D. A. Forsyth, J. Malik, M. M. Fleck, H. Greenspan, T. Leung, S. Belongie, C. Carson, and C. Bregler. Finding pictures of objects in large collections of images. In *International workshop on object representation in computer vision*, pages 335–360. Springer, 1996.
- [18] M. Gardner, Y. Artzi, V. Basmov, J. Berant, B. Bogin, S. Chen, P. Dasigi, D. Dua, Y. Elazar, A. Gottumukkala, et al. Evaluating models’ local decision boundaries via contrast sets. In *Proceedings of the 2020 Conference on Empirical Methods in Natural Language Processing: Findings*, pages 1307–1323, 2020.
- [19] R. Geirhos, P. Rubisch, C. Michaelis, M. Bethge, F. A. Wichmann, and W. Brendel. Imagenet-trained cnns are biased towards texture; increasing shape bias improves accuracy and robustness. *arXiv preprint arXiv:1811.12231*, 2018.
- [20] R. Geirhos, J.-H. Jacobsen, C. Michaelis, R. Zemel, W. Brendel, M. Bethge, and F. A. Wichmann. Shortcut learning in deep neural networks. *Nature Machine Intelligence*, 2(11):665–673, 2020.
- [21] I. Gulrajani and D. Lopez-Paz. In search of lost domain generalization. *arXiv preprint arXiv:2007.01434*, 2020.
- [22] C. Guo, G. Pleiss, Y. Sun, and K. Q. Weinberger. On calibration of modern neural networks. In *International Conference on Machine Learning*, pages 1321–1330. PMLR, 2017.
- [23] R. Hamon, H. Junklewitz, and I. Sanchez. Robustness and explainability of artificial intelligence. *Publications Office of the European Union*, 2020.
- [24] K. He, X. Zhang, S. Ren, and J. Sun. Deep residual learning for image recognition. In *Proceedings of the IEEE conference on computer vision and pattern recognition*, pages 770–778, 2016.
- [25] C. Heinze-Deml and N. Meinshausen. Conditional variance penalties and domain shift robustness. *Machine Learning*, 110(2):303–348, 2021.

- [26] G. Heitz and D. Koller. Learning spatial context: Using stuff to find things. In *European conference on computer vision*, pages 30–43. Springer, 2008.
- [27] D. Hendrycks and T. Dietterich. Benchmarking neural network robustness to common corruptions and perturbations. *arXiv preprint arXiv:1903.12261*, 2019.
- [28] D. Hendrycks and K. Gimpel. A baseline for detecting misclassified and out-of-distribution examples in neural networks. *arXiv preprint arXiv:1610.02136*, 2016.
- [29] D. Hendrycks, K. Zhao, S. Basart, J. Steinhardt, and D. Song. Natural adversarial examples. In *Proceedings of the IEEE/CVF Conference on Computer Vision and Pattern Recognition*, pages 15262–15271, 2021.
- [30] W. Hu, G. Niu, I. Sato, and M. Sugiyama. Does distributionally robust supervised learning give robust classifiers? In *International Conference on Machine Learning*, pages 2029–2037. PMLR, 2018.
- [31] P. Isabelle, C. Cherry, and G. Foster. A challenge set approach to evaluating machine translation. *arXiv preprint arXiv:1704.07431*, 2017.
- [32] J. Kaplan, S. McCandlish, T. Henighan, T. B. Brown, B. Chess, R. Child, S. Gray, A. Radford, J. Wu, and D. Amodei. Scaling laws for neural language models. *arXiv preprint arXiv:2001.08361*, 2020.
- [33] B. Kim, H. Kim, K. Kim, S. Kim, and J. Kim. Learning not to learn: Training deep neural networks with biased data. In *Proceedings of the IEEE/CVF Conference on Computer Vision and Pattern Recognition*, pages 9012–9020, 2019.
- [34] P. W. Koh, S. Sagawa, H. Marklund, S. M. Xie, M. Zhang, A. Balsubramani, W. Hu, M. Yasunaga, R. L. Phillips, I. Gao, et al. Wilds: A benchmark of in-the-wild distribution shifts. *arXiv preprint arXiv:2012.07421*, 2020.
- [35] D. Krueger, E. Caballero, J.-H. Jacobsen, A. Zhang, J. Binas, D. Zhang, R. L. Priol, and A. Courville. Out-of-distribution generalization via risk extrapolation (rex). *arXiv preprint arXiv:2003.00688*, 2020.
- [36] A. M. Larson, T. E. Freeman, R. V. Ringer, and L. C. Loschky. The spatiotemporal dynamics of scene gist recognition. *Journal of Experimental Psychology: Human Perception and Performance*, 40(2):471, 2014.
- [37] T.-Y. Lin, M. Maire, S. Belongie, J. Hays, P. Perona, D. Ramanan, P. Dollár, and C. L. Zitnick. Microsoft coco: Common objects in context. In *European conference on computer vision*, pages 740–755. Springer, 2014.
- [38] T.-Y. Lin, P. Goyal, R. Girshick, K. He, and P. Dollár. Focal loss for dense object detection. In *Proceedings of the IEEE international conference on computer vision*, pages 2980–2988, 2017.
- [39] C. Lovering, R. Jha, T. Linzen, and E. Pavlick. Predicting inductive biases of pre-trained models, 2021.
- [40] C. Michaelis, B. Mitzkus, R. Geirhos, E. Rusak, O. Bringmann, A. S. Ecker, M. Bethge, and W. Brendel. Benchmarking robustness in object detection: Autonomous driving when winter is coming. *arXiv preprint arXiv:1907.07484*, 2019.
- [41] K. Murphy, A. Torralba, W. Freeman, et al. Using the forest to see the trees: a graphical model relating features, objects and scenes. *Advances in neural information processing systems*, 16: 1499–1506, 2003.
- [42] A. Naik, A. Ravichander, N. Sadeh, C. Rose, and G. Neubig. Stress test evaluation for natural language inference. *arXiv preprint arXiv:1806.00692*, 2018.
- [43] C. Nebut, F. Fleurey, Y. Le Traon, and J.-M. Jezequel. Automatic test generation: A use case driven approach. *IEEE Transactions on Software Engineering*, 32(3):140–155, 2006.

- [44] A. Noack, I. Ahern, D. Dou, and B. Li. An empirical study on the relation between network interpretability and adversarial robustness. *SN Computer Science*, 2(1):1–13, 2021.
- [45] L. Oakden-Rayner, J. Dunnmon, G. Carneiro, and C. Ré. Hidden stratification causes clinically meaningful failures in machine learning for medical imaging. In *Proceedings of the ACM conference on health, inference, and learning*, pages 151–159, 2020.
- [46] A. Oliva and A. Torralba. Building the gist of a scene: The role of global image features in recognition. *Progress in brain research*, 155:23–36, 2006.
- [47] E. Perez, F. Strub, H. De Vries, V. Dumoulin, and A. Courville. Film: Visual reasoning with a general conditioning layer. In *Proceedings of the AAAI Conference on Artificial Intelligence*, volume 32, 2018.
- [48] J. Peters, P. Bühlmann, and N. Meinshausen. Causal inference by using invariant prediction: identification and confidence intervals. *Journal of the Royal Statistical Society. Series B (Statistical Methodology)*, pages 947–1012, 2016.
- [49] N. Reimers and I. Gurevych. Sentence-bert: Sentence embeddings using siamese bert-networks. *arXiv preprint arXiv:1908.10084*, 2019.
- [50] R. T. Rockafellar and S. Uryasev. Conditional value-at-risk for general loss distributions. *Journal of banking & finance*, 26(7):1443–1471, 2002.
- [51] A. Rosenfeld, R. Zemel, and J. K. Tsotsos. The elephant in the room. *arXiv preprint arXiv:1808.03305*, 2018.
- [52] A. Ross and F. Doshi-Velez. Improving the adversarial robustness and interpretability of deep neural networks by regularizing their input gradients. In *Proceedings of the AAAI Conference on Artificial Intelligence*, volume 32, 2018.
- [53] D. Rothenhäusler, N. Meinshausen, P. Bühlmann, and J. Peters. Anchor regression: heterogeneous data meets causality. *arXiv preprint arXiv:1801.06229*, 2018.
- [54] O. Russakovsky, J. Deng, H. Su, J. Krause, S. Satheesh, S. Ma, Z. Huang, A. Karpathy, A. Khosla, M. Bernstein, et al. Imagenet large scale visual recognition challenge. *International journal of computer vision*, 115(3):211–252, 2015.
- [55] S. Sagawa, P. W. Koh, T. B. Hashimoto, and P. Liang. Distributionally robust neural networks for group shifts: On the importance of regularization for worst-case generalization. *arXiv preprint arXiv:1911.08731*, 2019.
- [56] S. Santurkar, D. Tsipras, and A. Madry. Breeds: Benchmarks for subpopulation shift. *arXiv preprint arXiv:2008.04859*, 2020.
- [57] H. Shah, K. Tamuly, A. Raghunathan, P. Jain, and P. Netrapalli. The pitfalls of simplicity bias in neural networks. *arXiv preprint arXiv:2006.07710*, 2020.
- [58] R. Shetty, B. Schiele, and M. Fritz. Not using the car to see the sidewalk—quantifying and controlling the effects of context in classification and segmentation. In *Proceedings of the IEEE/CVF Conference on Computer Vision and Pattern Recognition*, pages 8218–8226, 2019.
- [59] M. Srivastava, T. Hashimoto, and P. Liang. Robustness to spurious correlations via human annotations. In *International Conference on Machine Learning*, pages 9109–9119. PMLR, 2020.
- [60] A. Torralba. Contextual priming for object detection. *International journal of computer vision*, 53(2):169–191, 2003.
- [61] E. Triantafillou, H. Larochelle, R. Zemel, and V. Dumoulin. Learning a universal template for few-shot dataset generalization. *arXiv preprint arXiv:2105.07029*, 2021.

- [62] J. K. Winkler, C. Fink, F. Toberer, A. Enk, T. Deinlein, R. Hofmann-Wellenhof, L. Thomas, A. Lallas, A. Blum, W. Stolz, et al. Association between surgical skin markings in dermoscopic images and diagnostic performance of a deep learning convolutional neural network for melanoma recognition. *JAMA dermatology*, 155(10):1135–1141, 2019.
- [63] K. Wu, E. Wu, and G. Kreiman. Learning scene gist with convolutional neural networks to improve object recognition. In *2018 52nd Annual Conference on Information Sciences and Systems (CISS)*, pages 1–6. IEEE, 2018.
- [64] K. Xiao, L. Engstrom, A. Ilyas, and A. Madry. Noise or signal: The role of image backgrounds in object recognition. *arXiv preprint arXiv:2006.09994*, 2020.
- [65] S. M. Xie, A. Kumar, R. Jones, F. Khani, T. Ma, and P. Liang. In-n-out: Pre-training and self-training using auxiliary information for out-of-distribution robustness. *arXiv preprint arXiv:2012.04550*, 2020.
- [66] B. Yao and L. Fei-Fei. Modeling mutual context of object and human pose in human-object interaction activities. In *2010 IEEE Computer Society Conference on Computer Vision and Pattern Recognition*, pages 17–24. IEEE, 2010.

A Other Methods

We detail a few other methods which we explored but do not include for analysis in Sec. 6:

- Logistic regression on pre-trained Imagenet features: We found this performed noticeably worse than ERM across the board, with a slight improvement in loss on hard positives (but worse than most other methods).
- ERM trained from scratch: We found this to perform slightly worse across the board than ERM from a pre-trained model.
- ERM with learning rate decay: We explored several learning rate decays and found, with tuning, minor improvements in overall performance from ERM. Due to the level of tuning required, we chose not to include these results and just used a constant learning rate.
- ERM with data augmentation: We explored using data augmentations such as random affine transformations, cropping, and horizontal flips, but found they did not improve performance in ERM.
- Adaptive parameters [47, 61]: We explored the possibility of learning affine transformations after each ResNet block. With tuning, we found this improved performance on hard examples over ERM but not close to the level of the other robust methods shown.
- Auxiliary prediction: We explored adding a second readout head to the final layer and predicting the highest α -context variable as an auxiliary loss. We found this to perform nearly identically to ERM in all metrics, and occasionally slightly worse.

We include this list for completeness: this is not to say that no such approach can be useful for this problem, but at the time of writing we did not find compelling enough results from these methods to yield interesting or informative comparative analysis in Sec. 6.

B Data

B.1 Licences

- The images in the COCO dataset [37] are provided under the Flickr terms of use.
- The annotations in the COCO dataset [37] are provided under a Creative Commons Attribution 4.0 License.
- The annotations in the COCO-Stuff dataset [7] are provided under a Creative Commons Attribution 4.0 License.

B.2 Dataset Details

We use the COCO-Stuff dataset [7] (<https://github.com/nightrome/cocostuff>), which contains images and annotations from the COCO dataset [37], as well as adding additional annotations. Since COCO is a competitive benchmark, the test set is not publicly available, so we merge the provided training/validation sets and create our own new training/validation/test split using 70/10/20 percentages. This yields training/validation/test set sizes of 86302/12328/24657.

B.3 Creation of the NOOCH Suite

When choosing the tasks, we filtered out a couple of tasks which seemed subjectively too similar to ones already in the benchmark. Specifically, we removed `sheep`, `handbag`, `bottle`, and `wine-glass` due to the fact that other similar tasks had higher average difference in average NLL on all examples and average NLL on hard examples (specifically, `cow`, `backpack`, `cup`, and `cup` respectively). We also filtered out those tasks without at least 50 hard positives and hard negatives.

Fig 10 shows that, under the CE criterion, most of the 171 object classes in COCO-Stuff have context cues for $\alpha \geq 0$. Note that a 0-context cue is fairly strong: this means that on average, in images where Y is present, C takes up at least as much area as Y does. This indicates that there may be a large number of OOC examples hidden in many of these tasks. We find that the contexts returned using this method for large enough α are intuitive. Some examples of (label, 0.05-context) pairs are: (car,

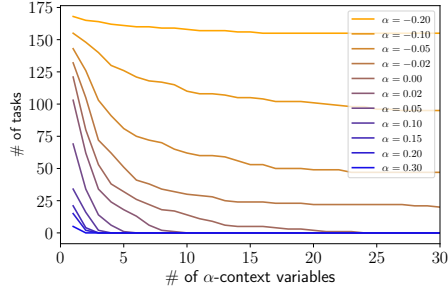


Figure 10: The number of tasks in the COCO-Stuff dataset which have context variables identifiable at each level of α . There are 171 total tasks. For instance, this figure shows that there are around 70 tasks with at least one context cue at $\alpha \geq 0.05$, and around 30 tasks with at least five context cues at $\alpha \geq 0$.

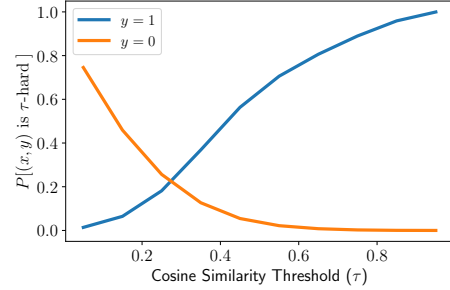


Figure 11: Using the gist criterion, the number of τ -hard positive/negative examples in the COCO-Stuff test set as a proportion of all positive/negative examples, where τ thresholds the cosine similarity to the average caption embedding of that category in the training set.

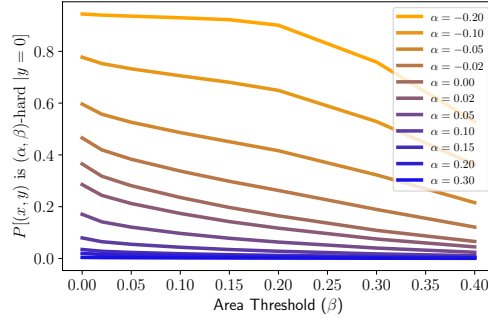
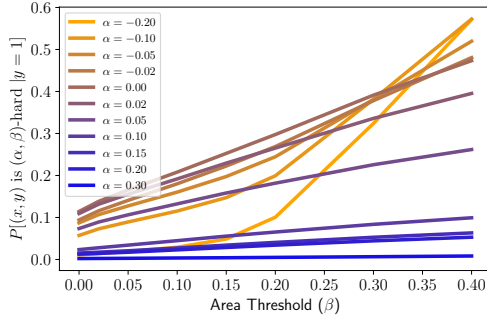


Figure 12: Across a range of α, β , the percentage of hard positive/negative examples (L/R) in the test set which are (α, β) -hard.

road), (bowl, dining_table), (cow, grass). Additionally, many tasks have more than one context variable: at $\alpha = 0$ about 50 tasks have 3, and at $\alpha = 0.05$ about 15 tasks have 3. Some examples of labels with multiple 0.05-context variables are: (surfboard, [sea, sky-other]), (tennis-racket, [person, playing-field]), (traffic-light, [building-other, road, sky-other, tree]). All of these groupings are intuitive, providing some evidence that this method of isolating context variables may be a useful one.

In Fig. 11 we see, across all values of τ , how many τ -hard examples there are in the test set by the gist criterion, across all 171 tasks in COCO-Stuff. As expected, the number of hard positives increases with τ , and the number of hard negatives decreased.

Fig 12 shows that hard positive/negative examples are numerous in the data. For instance, we see that at the (0.05, 0.1) level, about 10% of all possible (object, category) pairs are hard positives, and a similar number for hard negatives.

Fig. 13 shows the average loss incurred by (α, β) -hard positive and negative examples under the CE criterion as α, β vary.

Fig. 14 shows the average loss incurred by (τ) -hard positive and negative examples under the gist criterion as τ varies.

In the paper, we choose $\alpha, \beta = 0.05, 0.1$ for the CE criterion, and then set τ in each task such that the number of hard positive and negative examples in each task is the same. Tables 6 and 7 show these values of τ for each for the 12 NOOCH tasks.

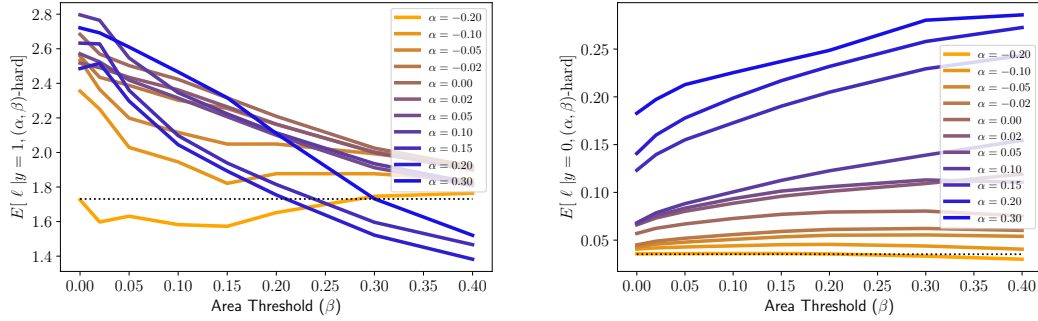


Figure 13: Across a range of α, β , the average test set loss of positive/negative examples (L/R) in the test set which are (α, β) -hard.

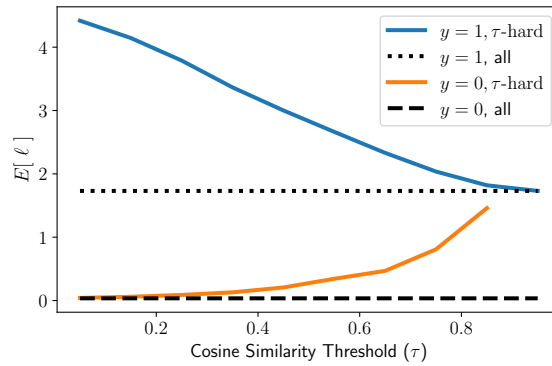


Figure 14: Caption

C Experimental Details

C.1 Licences

The Resnet-50 is provided under an Apache 2.0 licence.

Task	Hard Positives	Hard Negatives
car	0.48	0.48
bowl	0.64	0.57
boat	0.73	0.43
fire-hydrant	0.74	0.35
airplane	0.81	0.19
cow	0.73	0.24
backpack	0.39	0.3
cup	0.46	0.23
surfboard	0.66	0.21
tie	0.26	0.23
sports-ball	0.47	0.12
kite	0.57	0.19

Table 6: Values for τ used for the gist criterion throughout the paper (test set).

Task	Hard Positives	Hard Negatives
car	0.47	0.5
bowl	0.65	0.57
boat	0.72	0.42
fire-hydrant	0.76	0.35
airplane	0.81	0.19
cow	0.71	0.23
backpack	0.39	0.31
cup	0.46	0.23
surfboard	0.68	0.21
tie	0.25	0.23
sports-ball	0.44	0.12
kite	0.58	0.19

Table 7: Values for τ used for the gist criterion throughout the paper (validation set).

Method	Hyperparameter Name	Values
GDRO	K	[5, 30, 60, 240]
IRM	λ	[0.1, 1, 3, 10]
CVaR	p	[0.05, 0.1, 0.15]
Focal	γ	[0.2, 0.5, 0.7, 1]
Label Reweighting	α	[0.2, 0.5, 0.7, 1]
Label Undersampling	α	[0.2, 0.5, 0.7, 1]
Environment Reweighting	α	[0.5, 1, 1.5, 2]
Environment Undersampling	α	[0.2, 0.5, 0.7, 1]

Table 8: Hyperparameter lists for each method (ERM has no method-specific hyperparameters).

Task	ERM	CVaR	Focal	Reweight	US	Reweight (Evo)	US (Evo)	GDRO	IRM	Task	ERM	CVaR	Focal	Reweight	US	Reweight (Evo)	US (Evo)	GDRO	IRM
car	0.769 (0.002)	0.787 (0.007)	0.759 (0.006)	0.773 (0.003)	0.773 (0.003)	0.866 (0.002)	0.846 (0.013)	0.897 (0.006)	0.808 (0.002)	car	0.766 (0.002)	0.785 (0.003)	0.765 (0.003)	0.768 (0.005)	0.773 (0.006)	0.845 (0.001)	0.823 (0.000)	0.863 (0.008)	0.832 (0.007)
boat	0.759 (0.003)	0.781 (0.013)	0.734 (0.004)	0.775 (0.004)	0.759 (0.007)	0.864 (0.003)	0.814 (0.006)	0.865 (0.011)	0.828 (0.021)	boat	0.842 (0.004)	0.866 (0.015)	0.825 (0.002)	0.826 (0.006)	0.828 (0.007)	0.898 (0.006)	0.786 (0.013)	0.879 (0.011)	
bird	0.869 (0.002)	0.888 (0.018)	0.823 (0.005)	0.866 (0.004)	0.877 (0.006)	0.954 (0.002)	0.923 (0.002)	0.945 (0.012)	0.925 (0.004)	bird	0.826 (0.002)	0.855 (0.019)	0.771 (0.008)	0.823 (0.004)	0.823 (0.002)	0.897 (0.002)	0.868 (0.003)	0.884 (0.008)	0.872 (0.002)
fine-hydrant	0.913 (0.004)	0.933 (0.003)	0.908 (0.003)	0.927 (0.001)	0.913 (0.001)	0.920 (0.002)	0.940 (0.003)	0.942 (0.004)		fine-hydrant	0.940 (0.007)	0.956 (0.008)	0.822 (0.005)	0.940 (0.005)	0.941 (0.007)	0.934 (0.005)	0.936 (0.007)	0.923 (0.007)	0.948 (0.004)
airplane	0.986 (0.002)	0.984 (0.002)	0.981 (0.001)	0.986 (0.000)	0.985 (0.002)	0.991 (0.000)	0.986 (0.001)	0.991 (0.001)	0.986 (0.001)	airplane	0.977 (0.001)	0.979 (0.000)	0.975 (0.001)	0.978 (0.000)	0.976 (0.001)	0.978 (0.001)	0.976 (0.001)	0.981 (0.003)	0.977 (0.002)
cow	0.915 (0.003)	0.937 (0.003)	0.932 (0.001)	0.939 (0.001)	0.935 (0.001)	0.963 (0.001)	0.948 (0.002)	0.963 (0.004)	0.943 (0.011)	cow	0.901 (0.004)	0.912 (0.001)	0.877 (0.002)	0.901 (0.002)	0.906 (0.004)	0.908 (0.002)	0.908 (0.003)	0.911 (0.004)	0.906 (0.001)
backpack	0.812 (0.004)	0.806 (0.010)	0.809 (0.002)	0.816 (0.003)	0.812 (0.008)	0.813 (0.002)	0.816 (0.014)	0.871 (0.008)	0.844 (0.011)	backpack	0.716 (0.004)	0.717 (0.011)	0.725 (0.002)	0.731 (0.003)	0.749 (0.004)	0.729 (0.004)	0.736 (0.001)	0.732 (0.012)	0.750 (0.010)
cup	0.875 (0.004)	0.863 (0.008)	0.867 (0.001)	0.876 (0.000)	0.875 (0.000)	0.879 (0.006)	0.875 (0.001)	0.821 (0.019)	0.869 (0.020)	cup	0.731 (0.004)	0.738 (0.007)	0.727 (0.000)	0.738 (0.001)	0.742 (0.004)	0.779 (0.006)	0.771 (0.000)	0.742 (0.015)	0.758 (0.011)
surfboard	0.939 (0.002)	0.947 (0.002)	0.933 (0.001)	0.940 (0.001)	0.939 (0.001)	0.960 (0.001)	0.940 (0.002)	0.960 (0.004)	0.957 (0.008)	surfboard	0.913 (0.002)	0.920 (0.002)	0.906 (0.002)	0.912 (0.002)	0.914 (0.000)	0.909 (0.001)	0.912 (0.001)	0.882 (0.006)	0.904 (0.011)
tie	0.742 (0.002)	0.752 (0.008)	0.728 (0.006)	0.760 (0.005)	0.763 (0.009)	0.756 (0.006)	0.761 (0.003)	0.806 (0.015)	0.775 (0.028)	tie	0.823 (0.003)	0.816 (0.007)	0.811 (0.004)	0.829 (0.004)	0.824 (0.002)	0.831 (0.005)	0.835 (0.009)	0.840 (0.017)	
sports-ball	0.867 (0.002)	0.869 (0.007)	0.871 (0.001)	0.869 (0.002)	0.868 (0.006)	0.911 (0.001)	0.890 (0.002)	0.911 (0.005)	0.884 (0.001)	sports-ball	0.826 (0.003)	0.832 (0.009)	0.828 (0.001)	0.830 (0.002)	0.823 (0.004)	0.866 (0.003)	0.850 (0.002)	0.880 (0.011)	0.855 (0.011)
kite	0.932 (0.001)	0.932 (0.001)	0.937 (0.002)	0.940 (0.001)	0.928 (0.002)	0.949 (0.001)	0.936 (0.001)	0.969 (0.005)	0.950 (0.012)	kite	0.942 (0.001)	0.939 (0.005)	0.945 (0.002)	0.947 (0.001)	0.936 (0.003)	0.939 (0.002)	0.947 (0.007)	0.943 (0.010)	0.943 (0.010)
Average	0.865 (0.001)	0.874 (0.006)	0.857 (0.001)	0.870 (0.001)	0.867 (0.002)	0.905 (0.001)	0.888 (0.002)	0.911 (0.003)	0.897 (0.004)	Average	0.827 (0.001)	0.837 (0.003)	0.818 (0.001)	0.827 (0.001)	0.824 (0.001)	0.849 (0.001)	0.847 (0.001)	0.859 (0.001)	0.854 (0.001)

Table 9: AUC on hard test examples for all 12 NOOCH stress tests, after hyperparameter selection. Bold numbers have overlapping standard deviations. L: NOOCH-CE. R: NOOCH-Gist.

C.2 General Hyperparameters

We train (where not otherwise indicated) using SGD with learning rate of $1e-4$, momentum of 0.9, L2 weight regularization of $1e-4$, and batch size 32 (the largest we could fit on the available GPUs). For all methods, we use early stopping on the validation loss with a patience of 3 epochs. All images were resized to 321×321 .

Training Parameters for ERM in Sec. 3. For the experiments which refer to all 171 tasks (rather than just the 12 we focus on in NOOCH), we use an Adam optimizer with $1e-3$ learning rate and batch size 16. All other training parameters are the same as noted elsewhere.

Sentence Embeddings. To computer sentence embeddings, we use `stsb-distilroberta-base-v2` from the `sentence_transformers` package (<https://www.sbert.net/>).

C.3 Compute

We used GPUs on internal clusters, utilizing Nvidia Titan XP, T4, and P100 GPUs. The total number of jobs run to produce our main results, i.e. Table ?? and all associated figures, is

$$\text{num_tasks} \times \text{num_seeds} \times \text{num_methods} \times \text{num_hyperparameters_per_method} \quad (8)$$

$$= 12 \times 3 \times 5 \times 3.2 = 576 \quad (9)$$

where we calculate `num_hyperparameters_per_method` from Table 8. The job runtime lengths varied widely due to the use of early stopping.

C.4 Method-Specific Hyperparameters

Each of the methods we run other than ERM has a hyperparameter which trades off better overall performance and OOC performance. For each method, we swept over 4 values of these parameters (3 for CVaR), running 3 seeds at each value. The values of these hyperparameters are shown in Table 8. They were chosen through some manual experimentation to get a sense of the useful ranges for each.

C.5 Detailed Results

For each metric of AUC, NLL, Error, and ECE, each of the 12 tasks in NOOCH, and both NOOCH-CE and NOOCH-Gist, we show results below with standard deviation across 3 seeds. There are the same results as Figures 4, 5, 6, are 7, but shown in more detail.

Task	ERM	CVR	Fscal	Recweight	US	Recweight (Hans)	US (Tevs)	GDR0	HRM	ERM	CVR	Fscal	Recweight	US	Recweight (Hans)	US (Tevs)	GDR0	HRM	
car	0.988 (0.000)	0.987 (0.000)	0.986 (0.000)	0.988 (0.000)	0.987 (0.000)	0.989 (0.000)	0.987 (0.000)	0.987 (0.000)	0.987 (0.000)	0.988 (0.000)	0.987 (0.000)	0.986 (0.000)	0.988 (0.000)	0.987 (0.000)					
head	0.981 (0.000)	0.981 (0.000)	0.982 (0.000)	0.981 (0.000)	0.982 (0.000)	0.981 (0.000)													
boat	0.995 (0.000)																		
fire-hydrant	0.979 (0.001)																		
airplane	0.997 (0.001)																		
cow	0.995 (0.001)																		
airplane	0.992 (0.001)																		
backpack	0.992 (0.001)																		
cup	0.992 (0.001)																		
airplane	0.992 (0.001)																		
airplane	0.992 (0.001)																		
airplane	0.992 (0.001)																		
airplane	0.992 (0.001)																		
airplane	0.992 (0.001)																		
Average	0.988 (0.000)																		

Table 10: AUC on easy test examples for all 12 NOOCH stress tests, after hyperparameter selection. Bold numbers have overlapping standard deviations. L: NOOCH-CE. R: NOOCH-Gist.

Task	ERM	CVR	Fscal	Recweight	US	Recweight (Hans)	US (Tevs)	GDR0	HRM	ERM	CVR	Fscal	Recweight	US	Recweight (Hans)	US (Tevs)	GDR0	HRM	
car	0.448 (0.012)	0.476 (0.030)	0.197 (0.000)	0.301 (0.003)	0.377 (0.017)	0.251 (0.013)	0.368 (0.020)	0.136 (0.001)	0.257 (0.041)	car	0.459 (0.011)	0.495 (0.029)	0.207 (0.009)	0.321 (0.006)	0.380 (0.014)	0.279 (0.015)	0.386 (0.024)	0.257 (0.040)	0.278 (0.027)
head	0.581 (0.002)	0.627 (0.054)	0.162 (0.007)	0.336 (0.014)	0.408 (0.021)	0.314 (0.005)	0.309 (0.015)	0.239 (0.017)	0.286 (0.023)	head	0.416 (0.011)	0.670 (0.059)	0.178 (0.008)	0.370 (0.017)	0.443 (0.021)	0.405 (0.022)	0.416 (0.016)	0.300 (0.066)	0.276 (0.027)
boat	0.359 (0.009)	0.362 (0.028)	0.120 (0.009)	0.183 (0.002)	0.320 (0.002)	0.199 (0.002)	0.332 (0.002)	0.145 (0.020)	0.225 (0.055)	boat	0.419 (0.015)	0.458 (0.040)	0.129 (0.009)	0.211 (0.000)	0.357 (0.006)	0.283 (0.009)	0.400 (0.021)	0.211 (0.040)	0.361 (0.135)
fire-hydrant	0.460 (0.011)	0.468 (0.010)	0.181 (0.011)	0.217 (0.004)	0.418 (0.020)	0.381 (0.001)	0.397 (0.007)	0.268 (0.010)	0.268 (0.010)	fire-hydrant	0.442 (0.011)	0.468 (0.011)	0.181 (0.011)	0.217 (0.004)	0.418 (0.020)	0.381 (0.001)	0.397 (0.007)	0.268 (0.010)	0.268 (0.010)
airplane	0.117 (0.008)	0.125 (0.011)	0.054 (0.000)	0.054 (0.000)	0.112 (0.005)	0.103 (0.002)	0.114 (0.004)	0.056 (0.007)	0.090 (0.013)	airplane	0.200 (0.013)	0.186 (0.021)	0.097 (0.004)	0.097 (0.004)	0.177 (0.005)	0.168 (0.004)	0.177 (0.002)	0.098 (0.002)	0.116 (0.011)
cow	0.870 (0.009)	0.845 (0.017)	0.115 (0.008)	0.195 (0.002)	0.340 (0.013)	0.258 (0.005)	0.314 (0.009)	0.187 (0.010)	0.249 (0.015)	cow	0.758 (0.011)	0.826 (0.014)	0.144 (0.018)	0.240 (0.006)	0.426 (0.009)	0.366 (0.006)	0.431 (0.015)	0.268 (0.022)	0.280 (0.031)
airplane	0.823 (0.003)	0.883 (0.019)	0.239 (0.005)	0.237 (0.007)	0.538 (0.042)	0.599 (0.041)	0.638 (0.011)	0.238 (0.014)	0.271 (0.082)	airplane	0.801 (0.003)	0.919 (0.044)	0.318 (0.002)	0.318 (0.006)	0.666 (0.015)	0.688 (0.005)	0.715 (0.008)	0.340 (0.046)	0.337 (0.073)
cup	0.975 (0.011)	0.982 (0.010)	0.966 (0.001)	0.966 (0.000)	0.962 (0.001)	0.964 (0.001)	0.963 (0.001)	0.922 (0.017)	0.946 (0.016)	cup	0.999 (0.001)	0.989 (0.001)	0.995 (0.000)	0.995 (0.000)	0.991 (0.001)	0.989 (0.001)	0.984 (0.001)	0.989 (0.001)	0.979 (0.001)
airplane	0.372 (0.014)	0.388 (0.010)	0.184 (0.017)	0.172 (0.012)	0.435 (0.018)	0.184 (0.016)	0.315 (0.028)	0.164 (0.018)	0.220 (0.017)	airplane	0.317 (0.017)	0.342 (0.018)	0.213 (0.020)	0.216 (0.012)	0.449 (0.010)	0.367 (0.010)	0.497 (0.024)	0.329 (0.011)	0.423 (0.067)
cup	0.985 (0.003)	0.985 (0.003)	0.985 (0.003)	cup	0.985 (0.003)	0.985 (0.003)	0.985 (0.003)												
airplane	0.521 (0.022)	0.563 (0.018)	0.285 (0.014)	0.258 (0.009)	0.477 (0.017)	0.199 (0.000)	0.446 (0.010)	0.265 (0.063)	0.243 (0.049)	airplane	0.554 (0.017)	0.654 (0.070)	0.360 (0.008)	0.354 (0.005)	0.600 (0.010)	0.245 (0.014)	0.245 (0.014)	0.245 (0.014)	0.245 (0.014)
airplane	0.886 (0.004)	0.970 (0.011)	0.206 (0.000)	0.206 (0.000)	0.866 (0.000)	0.866 (0.000)	0.866 (0.000)	0.176 (0.042)	0.152 (0.017)	airplane	0.882 (0.004)	0.840 (0.017)	0.882 (0.004)						
airplane	0.955 (0.003)	0.953 (0.003)	0.953 (0.003)	airplane	0.955 (0.003)	0.953 (0.003)	0.953 (0.003)												
Average	0.633 (0.002)	0.633 (0.002)	0.285 (0.001)	0.165 (0.003)	0.361 (0.003)	0.168 (0.002)	0.361 (0.002)	0.136 (0.000)	0.154 (0.014)	Average	0.641 (0.002)	0.638 (0.002)	0.338 (0.004)	0.214 (0.003)	0.683 (0.004)	0.616 (0.003)	0.607 (0.001)	0.198 (0.011)	0.238 (0.015)

Table 11: Classification error on hard positive test examples for all 12 NOOCH stress tests, after hyperparameter selection. Bold numbers have overlapping standard deviations. L: NOOCH-CE. R: NOOCH-Gist.

Task	ERM	CVR	Fscal	Recweight	US	Recweight (Hans)	US (Tevs)	GDR0	HRM	ERM	CVR	Fscal	Recweight	US	Recweight (Hans)	US (Tevs)	GDR0	HRM	
car	0.115 (0.009)	0.884 (0.015)	0.884 (0.015)	0.829 (0.006)	0.155 (0.002)	0.152 (0.005)	0.152 (0.005)	0.186 (0.012)	0.155 (0.015)	car	0.115 (0.008)	0.886 (0.016)	0.821 (0.016)	0.826 (0.009)	0.817 (0.020)	0.156 (0.004)	0.125 (0.011)	0.181 (0.018)	0.241 (0.011)
head	0.087 (0.016)																		

Task	ERM	CVaR	Focal	Resweight	US	Resweight (Evo)	US (Evo)	GERO	ERM	Task	ERM	CVaR	Focal	Resweight	US	Resweight (Evo)	US (Evo)	GERO	ERM
car	0.017 (0.001)	0.005 (0.002)	0.004 (0.000)	0.017 (0.000)	0.015 (0.002)	0.004 (0.000)	0.014 (0.001)	0.008 (0.001)	0.002 (0.001)	car	0.019 (0.001)	0.006 (0.002)	0.003 (0.000)	0.013 (0.001)	0.016 (0.002)	0.005 (0.000)	0.015 (0.001)	0.006 (0.000)	0.002 (0.001)
boat	0.015 (0.001)	0.011 (0.000)	0.007 (0.001)	0.009 (0.000)	0.010 (0.002)	0.004 (0.000)	0.009 (0.002)	0.006 (0.002)	0.005 (0.001)	boat	0.015 (0.001)	0.008 (0.001)	0.014 (0.001)	0.014 (0.000)	0.014 (0.001)	0.013 (0.000)	0.014 (0.002)	0.005 (0.001)	0.004 (0.001)
boat	0.004 (0.000)	0.002 (0.000)	0.007 (0.001)	0.004 (0.000)	0.004 (0.000)	0.001 (0.000)	0.004 (0.000)	0.002 (0.000)	0.005 (0.001)	boat	0.005 (0.000)	0.003 (0.000)	0.009 (0.001)	0.006 (0.000)	0.005 (0.000)	0.004 (0.000)	0.002 (0.000)	0.002 (0.001)	0.002 (0.000)
fire-hydrant	0.002 (0.000)	0.001 (0.000)	0.003 (0.000)	0.001 (0.000)	0.002 (0.000)	0.001 (0.000)	0.002 (0.000)	0.004 (0.001)	0.001 (0.000)	fire-hydrant	0.003 (0.000)	0.001 (0.000)	0.004 (0.001)	0.004 (0.001)	0.003 (0.000)	0.002 (0.000)	0.003 (0.000)	0.001 (0.000)	0.001 (0.000)
airplane	0.001 (0.000)	0.000 (0.000)	0.010 (0.001)	0.005 (0.001)	0.001 (0.000)	0.001 (0.000)	0.001 (0.000)	0.001 (0.001)	0.001 (0.000)	airplane	0.001 (0.000)	0.001 (0.000)	0.009 (0.001)	0.004 (0.001)	0.001 (0.000)	0.000 (0.000)	0.001 (0.000)	0.003 (0.001)	0.008 (0.004)
cow	0.002 (0.000)	0.002 (0.000)	0.009 (0.000)	0.001 (0.000)	0.002 (0.000)	0.001 (0.000)	0.001 (0.000)	0.002 (0.000)	0.001 (0.000)	cow	0.002 (0.000)	0.002 (0.000)	0.006 (0.000)	0.004 (0.000)	0.003 (0.000)	0.002 (0.000)	0.001 (0.000)	0.001 (0.000)	0.001 (0.000)
backpack	0.006 (0.001)	0.018 (0.003)	0.009 (0.001)	0.022 (0.001)	0.008 (0.003)	0.002 (0.001)	0.004 (0.000)	0.007 (0.003)	0.011 (0.003)	backpack	0.008 (0.000)	0.016 (0.003)	0.005 (0.001)	0.018 (0.001)	0.014 (0.002)	0.004 (0.000)	0.007 (0.002)	0.011 (0.003)	0.012 (0.000)
cup	0.009 (0.001)	0.113 (0.002)	0.012 (0.001)	0.018 (0.001)	0.009 (0.002)	0.018 (0.002)	0.001 (0.000)	0.021 (0.011)	0.014 (0.004)	cup	0.008 (0.002)	0.105 (0.003)	0.000 (0.000)	0.046 (0.002)	0.015 (0.001)	0.020 (0.001)	0.007 (0.002)	0.012 (0.002)	0.016 (0.006)
surfboard	0.002 (0.000)	0.001 (0.000)	0.013 (0.001)	0.004 (0.000)	0.002 (0.000)	0.006 (0.001)	0.001 (0.000)	0.004 (0.001)	0.005 (0.001)	surfboard	0.002 (0.000)	0.001 (0.000)	0.006 (0.001)	0.005 (0.000)	0.003 (0.000)	0.005 (0.001)	0.002 (0.000)	0.003 (0.000)	0.017 (0.003)
tie	0.002 (0.000)	0.019 (0.004)	0.027 (0.002)	0.010 (0.001)	0.001 (0.000)	0.001 (0.000)	0.001 (0.000)	0.009 (0.002)	0.023 (0.007)	tie	0.002 (0.000)	0.017 (0.005)	0.023 (0.002)	0.006 (0.001)	0.003 (0.000)	0.001 (0.000)	0.003 (0.000)	0.013 (0.003)	0.025 (0.007)
sports-ball	0.002 (0.000)	0.023 (0.006)	0.028 (0.002)	0.017 (0.001)	0.006 (0.000)	0.002 (0.001)	0.021 (0.004)	0.035 (0.005)	0.025 (0.005)	sports-ball	0.004 (0.001)	0.023 (0.007)	0.028 (0.002)	0.023 (0.000)	0.002 (0.000)	0.035 (0.003)	0.002 (0.000)	0.014 (0.003)	0.028 (0.005)
kite	0.002 (0.000)	0.001 (0.000)	0.012 (0.001)	0.002 (0.000)	0.000 (0.000)	0.001 (0.000)	0.002 (0.001)	0.005 (0.002)	0.002 (0.000)	kite	0.001 (0.000)	0.001 (0.000)	0.011 (0.001)	0.002 (0.000)	0.000 (0.000)	0.001 (0.000)	0.002 (0.001)	0.002 (0.001)	0.005 (0.002)
Average	0.007 (0.000)	0.002 (0.001)	0.012 (0.001)	0.005 (0.000)	0.007 (0.000)	0.001 (0.000)	0.007 (0.000)	0.011 (0.002)	0.007 (0.001)	Average	0.007 (0.000)	0.002 (0.001)	0.012 (0.001)	0.005 (0.000)	0.007 (0.000)	0.006 (0.000)	0.007 (0.000)	0.010 (0.001)	0.009 (0.001)

Table 17: ECE on hard test examples for all 12 NOOCH stress tests, after hyperparameter selection. Bold numbers have overlapping standard deviations. L: NOOCH-CE. R: NOOCH-Gist.

Task	ERM	CVaR	Focal	Resweight	US	Resweight (Evo)	US (Evo)	GERO	ERM	Task	ERM	CVaR	Focal	Resweight	US	Resweight (Evo)	US (Evo)	GERO	ERM
car	0.006 (0.001)	0.188 (0.019)	0.147 (0.003)	0.016 (0.002)	0.009 (0.000)	0.007 (0.000)	0.011 (0.000)	0.116 (0.016)	0.004 (0.001)	car	0.010 (0.001)	0.189 (0.019)	0.147 (0.003)	0.016 (0.002)	0.011 (0.000)	0.120 (0.016)	0.125 (0.014)	0.012 (0.000)	0.006 (0.001)
boat	0.007 (0.001)	0.395 (0.001)	0.130 (0.002)	0.012 (0.001)	0.009 (0.005)	0.047 (0.003)	0.012 (0.008)	0.125 (0.029)	0.057 (0.016)	boat	0.009 (0.001)	0.398 (0.001)	0.137 (0.002)	0.017 (0.001)	0.012 (0.005)	0.044 (0.004)	0.015 (0.011)	0.117 (0.030)	0.113 (0.036)
boat	0.002 (0.000)	0.023 (0.003)	0.185 (0.003)	0.014 (0.002)	0.005 (0.000)	0.119 (0.002)	0.040 (0.001)	0.091 (0.026)	0.119 (0.007)	boat	0.003 (0.000)	0.023 (0.003)	0.187 (0.003)	0.017 (0.002)	0.004 (0.000)	0.120 (0.002)	0.004 (0.001)	0.095 (0.028)	0.079 (0.054)
fire-hydrant	0.001 (0.000)	0.016 (0.005)	0.151 (0.003)	0.010 (0.001)	0.002 (0.000)	0.011 (0.000)	0.003 (0.002)	0.069 (0.015)	0.069 (0.009)	fire-hydrant	0.002 (0.000)	0.016 (0.006)	0.157 (0.004)	0.014 (0.001)	0.003 (0.000)	0.011 (0.000)	0.004 (0.000)	0.069 (0.015)	0.072 (0.010)
airplane	0.001 (0.000)	0.002 (0.000)	0.032 (0.002)	0.015 (0.002)	0.000 (0.000)	0.004 (0.000)	0.001 (0.000)	0.020 (0.004)	0.004 (0.001)	airplane	0.001 (0.000)	0.002 (0.000)	0.034 (0.002)	0.016 (0.002)	0.001 (0.000)	0.004 (0.000)	0.001 (0.000)	0.028 (0.001)	0.032 (0.014)
cow	0.000 (0.000)	0.013 (0.005)	0.119 (0.003)	0.007 (0.000)	0.001 (0.000)	0.007 (0.000)	0.001 (0.000)	0.044 (0.016)	0.013 (0.001)	cow	0.001 (0.000)	0.013 (0.005)	0.126 (0.003)	0.009 (0.000)	0.001 (0.000)	0.008 (0.000)	0.006 (0.000)	0.036 (0.015)	0.037 (0.018)
backpack	0.001 (0.000)	0.308 (0.001)	0.098 (0.002)	0.010 (0.002)	0.005 (0.002)	0.016 (0.002)	0.006 (0.007)	0.085 (0.009)	0.042 (0.026)	backpack	0.007 (0.000)	0.310 (0.002)	0.142 (0.002)	0.025 (0.001)	0.006 (0.003)	0.021 (0.002)	0.012 (0.007)	0.079 (0.013)	0.099 (0.022)
cup	0.001 (0.001)	0.295 (0.005)	0.048 (0.005)	0.004 (0.001)	0.001 (0.001)	0.027 (0.003)	0.006 (0.004)	0.080 (0.015)	0.068 (0.002)	cup	0.007 (0.001)	0.303 (0.002)	0.128 (0.003)	0.027 (0.002)	0.007 (0.002)	0.065 (0.004)	0.009 (0.003)	0.110 (0.022)	0.091 (0.018)
surfboard	0.001 (0.000)	0.004 (0.001)	0.081 (0.005)	0.009 (0.001)	0.001 (0.000)	0.052 (0.009)	0.001 (0.000)	0.023 (0.003)	0.018 (0.002)	surfboard	0.001 (0.000)	0.004 (0.001)	0.051 (0.001)	0.010 (0.001)	0.001 (0.000)	0.053 (0.008)	0.001 (0.000)	0.025 (0.002)	0.057 (0.017)
tie	0.002 (0.000)	0.097 (0.018)	0.167 (0.011)	0.013 (0.003)	0.002 (0.000)	0.068 (0.001)	0.001 (0.000)	0.077 (0.023)	0.131 (0.016)	tie	0.001 (0.000)	0.098 (0.016)	0.128 (0.012)	0.028 (0.002)	0.002 (0.000)	0.099 (0.001)	0.001 (0.000)	0.068 (0.022)	0.120 (0.040)
sports-ball	0.000 (0.000)	0.042 (0.013)	0.127 (0.007)	0.018 (0.001)	0.002 (0.001)	0.112 (0.007)	0.004 (0.001)	0.053 (0.019)	0.071 (0.007)	sports-ball	0.003 (0.000)	0.044 (0.013)	0.135 (0.007)	0.025 (0.002)	0.003 (0.000)	0.117 (0.008)	0.005 (0.001)	0.062 (0.021)	0.080 (0.007)
kite	0.000 (0.000)	0.001 (0.000)	0.025 (0.002)	0.008 (0.001)	0.000 (0.000)	0.002 (0.000)	0.001 (0.000)	0.013 (0.004)	0.015 (0.005)	kite	0.000 (0.000)	0.001 (0.000)	0.029 (0.002)	0.010 (0.001)	0.000 (0.000)	0.002 (0.000)	0.000 (0.000)	0.013 (0.004)	0.014 (0.005)
Average	0.003 (0.000)	0.116 (0.004)	0.109 (0.001)	0.011 (0.000)	0.001 (0.001)	0.109 (0.001)	0.004 (0.001)	0.065 (0.008)	0.055 (0.004)	Average	0.004 (0.000)	0.118 (0.004)	0.116 (0.001)	0.018 (0.000)	0.004 (0.001)	0.044 (0.001)	0.006 (0.001)	0.071 (0.007)	0.069 (0.010)

Table 18: ECE on easy test examples for all 12 NOOCH stress tests, after hyperparameter selection. Bold numbers have overlapping standard deviations. L: NOOCH-CE. R: NOOCH-Gist.



Figure 15: Examples from the car task.



Figure 16: Examples from the bowl task.



Figure 17: Examples from the fire_hydrant task.



Figure 18: Examples from the airplane task.

D Qualitative Analysis

D.1 Examples

Here we show examples from NOOCH-CE: from left to right we show a hard positive, hard negative, and easy positive for each of the 12 tasks. We show the loss for a sample ERM model in the title of the caption. We choose these examples by finding the highest (lowest) loss ERM examples for each hard (easy) category — additionally, for ease of viewing, for hard positives, we choose examples for which the target object’s area is larger than average for positive examples of that class. We note that label noise can be a problem in COCO, as in any dataset, and finding the highest loss examples can occasionally surface a mislabelled datapoint (see Fig. 23, the Hard Negative in the tie class, where a tie is present but is not labelled). Along with subjectivity in labels, mislabelling is an occasional hazard of any dataset requiring mass labelling — fortunately, we did not find too many occurrences of mislabelled points when examining hard positives and negatives in NOOCH.

Hard Positive (cow): Loss = 6.98



Hard Negative (cow): Loss = 3.49



Easy Positive (cow): Loss = 0.00



Figure 19: Examples from the cow task.

Hard Positive (backpack): Loss = 5.49



Hard Negative (backpack): Loss = 2.92



Easy Positive (backpack): Loss = 0.00



Figure 20: Examples from the backpack task.

Hard Positive (cup): Loss = 5.37



Hard Negative (cup): Loss = 4.58



Easy Positive (cup): Loss = 0.00



Figure 21: Examples from the cup task.

Hard Positive (surfboard): Loss = 8.32



Hard Negative (surfboard): Loss = 5.01



Easy Positive (surfboard): Loss = 0.00



Figure 22: Examples from the surfboard task.

Hard Positive (tie): Loss = 8.08



Hard Negative (tie): Loss = 7.96



Easy Positive (tie): Loss = 0.00



Figure 23: Examples from the tie task.

D.2 Analyzing GDRO's Errors

In Fig. 8, we show the images with the largest gaps in NLL on the car task among two groups: hard positives and hard negatives (in NOOCH-CE), where GDRO is better than ERM. Here, in Fig. 26 we look at the images where GDRO most underperforms ERM. These help us consider some pitfalls

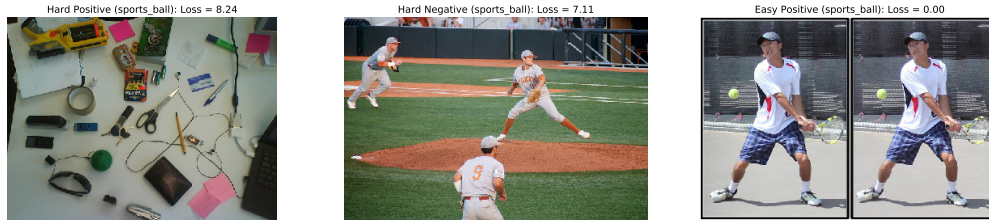


Figure 24: Examples from the `sports_ball` task.



Figure 25: Examples from the `kite` task.

of the GDRO objective, which incentivizes performance on two small subgroups: “cars without roads” and “roads without cars”. GDRO’s worst hard positive is reminiscent of a “road without a car”: the background (labelled “pavement”) looks road-like but the focal object is not a prototypical car (the car is in the top left, background). We hypothesize that GDRO’s incentive to perform well on “roads without cars” pushed its prediction negative, whereas ERM was able to take advantage of context and correctly output a positive. GDRO’s worst hard negative tells an opposite story: the snowy background looks *less* road-like, but the stop sign and black objects in the snow suggest a car may be present. We hypothesize that GDRO’s incentive to perform well on “cars without roads”, may have pushed its prediction wrongly *positive* in this instance.

Qualitatively, it appears that GDRO uses context in potentially more unintuitive ways than ERM does. While we hope that robust methods will be more interpretable since they may ignore irrelevant signals in the training data [23, 44, 52], these two goals may sometimes be at odds. Indeed, we observe that robust objectives may *unnecessarily* encourage predictions which diverge from the context.

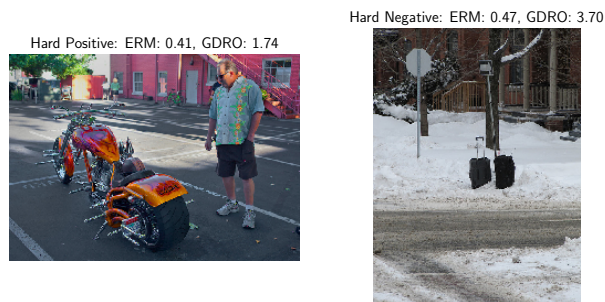


Figure 26: Test set examples with largest difference in NLL between ERM and GDRO methods, where ERM is better, among (L) hard positives and (R) hard negatives from the NOOCH-CE car category. Titles show NLL for each method on that image.